Geological Society of America
Memoir 163
1985

A multiple microfossil biochronology for the Miocene

John A. Barron
*Gerta Keller**
U.S. Geological Survey
345 Middlefield Road
Menlo Park, California 94025

Dean A. Dunn
Graduate School of Oceanography
University of Rhode Island
Narragansett, Rhode Island 02882
and
University of Southern Mississippi
Hattiesburg, Mississippi 39406

ABSTRACT

A multiple microfossil biochronology is presented for the Miocene which allows resolution of time approaching 100,000 years. Carbonate stratigraphy is integrated to greatly enhance this resolution. Graphical correlation techniques were applied to over 20 DSDP (Deep Sea Drilling Project) sections to identify 175 planktonic foraminiferal, calcareous nannofossil, radiolarian, and diatom datum levels between 24.0 and 4.3 Ma which show the most consistent (isochronous) correlations. Ages are estimated for these datum levels through 72 direct correlations to paleomagnetic stratigraphy and extrapolation between the correlation points. The resulting Miocene time scale resembles previously published time scales except for the early Miocene, where recent paleomagnetic correlations result in changes.

The three CENOP (Cenozoic Paleoceanography Project) time slices (~21, 16, and 8 Ma) are characterized biostratigraphically (planktonic foraminifers, calcareous nannofossils, radiolarians, and diatoms) and in terms of carbonate stratigraphy. The ages of the time slices are estimated as follows: the early Miocene time slice (21.2–20.1 Ma; given as 22 Ma in this volume), the late early Miocene time slice (16.4–15.2 Ma), and the late Miocene time slice (8.9–8.2 Ma).

An alternate time scale utilizing a paleomagnetic Anomaly 5-paleomagnetic Chron 11 correlation is also presented. Estimated ages for microfossil zones and datum levels in the late middle and early late Miocene (14–7 Ma) utilizing the alternate time scale are generally younger than those for the more traditional time scale. The late Miocene time slice has an estimated age of 8.0–7.0 Ma.

INTRODUCTION

During the past five years CENOP (Cenozoic Paleoceanography Project) workers have accumulated much detailed biostratigraphic and paleoecologic data on Miocene planktonic foraminifers (Srinivasan and Kennett, 1981a, b; Keller, 1980a, b, 1981a, b; Keller and Barron, 1981; Poore, 1981; Thunell, 1981; Vincent, 1981a), calcareous nannofossils (Haq et al., 1980); radiolarians (Moore and Lombari, 1981; Dunn, 1982; Romine, this volume); and diatoms (Burckle et al., 1982; Barron, 1983, in press; Barron and Keller, 1983; Burckle and Opdyke, this vol-

*Present address: Department of Geological and Geophysical Science, Princeton University, Princeton, New Jersey 08540.

ume). At the same time Dunn and Moore (1981), and Vincent, 1981b have developed a very detailed carbonate stratigraphy for the Miocene of the equatorial and central North Pacific which allows much greater time resolution than is possible with microfossil stratigraphies alone. These multiple microfossil and carbonate stratigraphies have been completed in as many deep-sea sequences as recovery and preservation permitted, including over 20 Miocene sequences from the Pacific Ocean (see map in volume preface). Among these latter sections, the most complete and representative biostratigraphic records are those from DSDP Sites 71 and 77 in the central equatorial Pacific and DSDP Site 289 in the western equatorial Pacific (Keller and Barron, 1983; Keller, 1981a; Saito, 1977; Ryan et al., 1974). These sites provide an excellent opportunity for correlation and integration of multiple microfossil datum events and carbonate stratigraphy and, hence, for the development of a high resolution stratigraphy for the Miocene. The expanding data base for direct ties of microfossil datum levels to paleomagnetic stratigraphy (Saito et al., 1975; Theyer et al., 1978; Burckle, 1978; Poore et al., 1983) allows correlation of this high resolution stratigraphy to radiometric time and the development of a refined Miocene chronostratigraphy (Keller et al., 1982).

The main purpose of this paper is to summarize these varied biostratigraphic data and to synthesize a high-resolution biochronology for the Miocene, based on microfossil datum events and carbonate events that are calibrated to the paleomagnetic time scale of Berggren et al. (1984). To achieve this goal we have combined microfossil datum events that are tied directly to paleomagnetic stratigraphy (Gartner, 1973; Saito et al., 1975; Burckle, 1978; Theyer et al., 1978; Poore et al., 1983) with our data set to test their isochroneity in DSDP sections analyzed in the Pacific Ocean, particularly Sites 71, 77, and 289. This approach has resulted in a reliable biochronologic model for the Miocene which yields an age resolution approaching 100,000 years. The second purpose of this paper is to define biostratigraphically the three time-slice intervals at about 21, 16, and 8 Ma which have been chosen by CENOP workers to study the paleoceanographic and paleoclimatic history of the Miocene ocean.

MIOCENE CHRONOSTRATIGRAPHY

A Miocene Time Scale

Correlation of the various low-latitude microfossil zones of the Miocene with the paleomagnetic time scale of Berggren et al. (1984) is shown in Figure 1. This figure incorporates the planktonic foraminiferal zones of Blow (1969) with subzones suggested by Srinivasan and Kennett (1981a, b) and Keller (in press), the calcareous nannofossil zones of Martini (1971) and Bukry (1973, 1975) (notation after Okada and Bukry, 1980), the radiolarian zones of Riedel and Sanfilippo (1978), and the diatom zones of Burckle (1972) and Barron (1983, in press). In addition, intervals of widespread deep-sea hiatuses (Keller and Barron, 1983) and the carbonate curves of DSDP Sites 158 (4.5–12.9 Ma) (Dunn and Moore, 1981) and 71 (12.0–22.0 Ma) (D. Dunn, unpublished data) are included to show their relationship with the microfossil stratigraphies. The main differences between this and earlier Miocene time scales (Ryan et al., 1974; Berggren, 1981) are in the early Miocene, where new paleomagnetic correlations (Poore et al., 1983; Barron et al., in press) have resulted in changes.

Specifically, the N4/N5 planktonic foraminiferal zone boundary is correlated with mid paleomagnetic Chron 19 on the basis of comparisons with paleomagnetically tied radiolarian datum levels (Theyer et al., 1978) rather than lower Chron 20 (Berggren, 1981) or upper Chron 21 (Ryan et al., 1974; Berggren et al., 1983). Berggren et al.'s (1983) correlation of the last occurrence of the planktonic foraminifer *Globorotalia kugleri* (= N4/N5 boundary) relies on his interpretation of the paleomagnetic Anomaly 6C at DSDP Site 516. His interpretation of Anomaly 6C is based on the first occurrence of *G. kugleri* at Site 516. However, that occurrence appears to be diachronously young based on the last occurrence of the calcareous nannofossil *Sphenolithus ciperoensis* (Berggren et al., 1983) and the first occurrence of the diatom *Rocella gelida* (Gombos, 1983) at the site. Within the tropics the last occurrences of *G kugleri* and *S. ciperoensis* are nearly coincident (Berggren et al., 1984; Barron et al., in press), and the first occurrence of *R. gelida* is immediately below those datum levels (Barron, 1983; Barron et al., in press).

In addition, the CN1/CN2 calcareous nannofossil zone boundary is herein tied with lower Chron 17 (Barron et al., in press) rather than with lower Chron 19 as proposed by Berggren (1981). Finally, the third major early Miocene difference involves the *Calocyletta costata/Stichocorys wolffii* radiolarian zone boundary. This boundary is placed in lower Chron 16 rather than mid Chron 17, as proposed by Berggren (1981), following the results of DSDP Leg 85 (Barron et al., in press) and reinterpretation of the paleomagnetic assignments of Theyer et al. (1978).

Following Berggren et al. (1984), the Oligocene/Miocene boundary is placed at 23.7 Ma in lower Anomaly 6C, which corresponds with the base of the calcareous nannofossil zones NN1 and CN1 and with the first occurrence of *Globorotalia kugleri* (the base of Zone N4 as recognized by Keller, in press). Other workers recognize the Oligocene/Miocene boundary at the top of calcareous nannofossil Subzone CN1a (Bukry, 1975; Keller and Barron, 1983) (22.7 Ma), the first occurrence of *Globigerinoides trilobus immaturus* or top of planktonic foraminiferal Subzone N4a (Keller, in press) (22.1 Ma), or the first occurrence of *Globoquadrina dehiscens,* which defines the top of planktonic foraminiferal Subzone N4b (21.2 Ma) (Srinivasan and Kennett, 1981a, b).

The early Miocene/middle Miocene boundary is placed at 16.0 Ma in the upper part of paleomagnetic Chron 16 within the lower part of planktonic foraminiferal Zone N8 and uppermost part of calcareous nannofossil zone NN4 following Ryan et al. (1974).

The middle Miocene/late Miocene boundary falls in the upper part of paleomagnetic Chron 11 at ~11.5 Ma in the middle

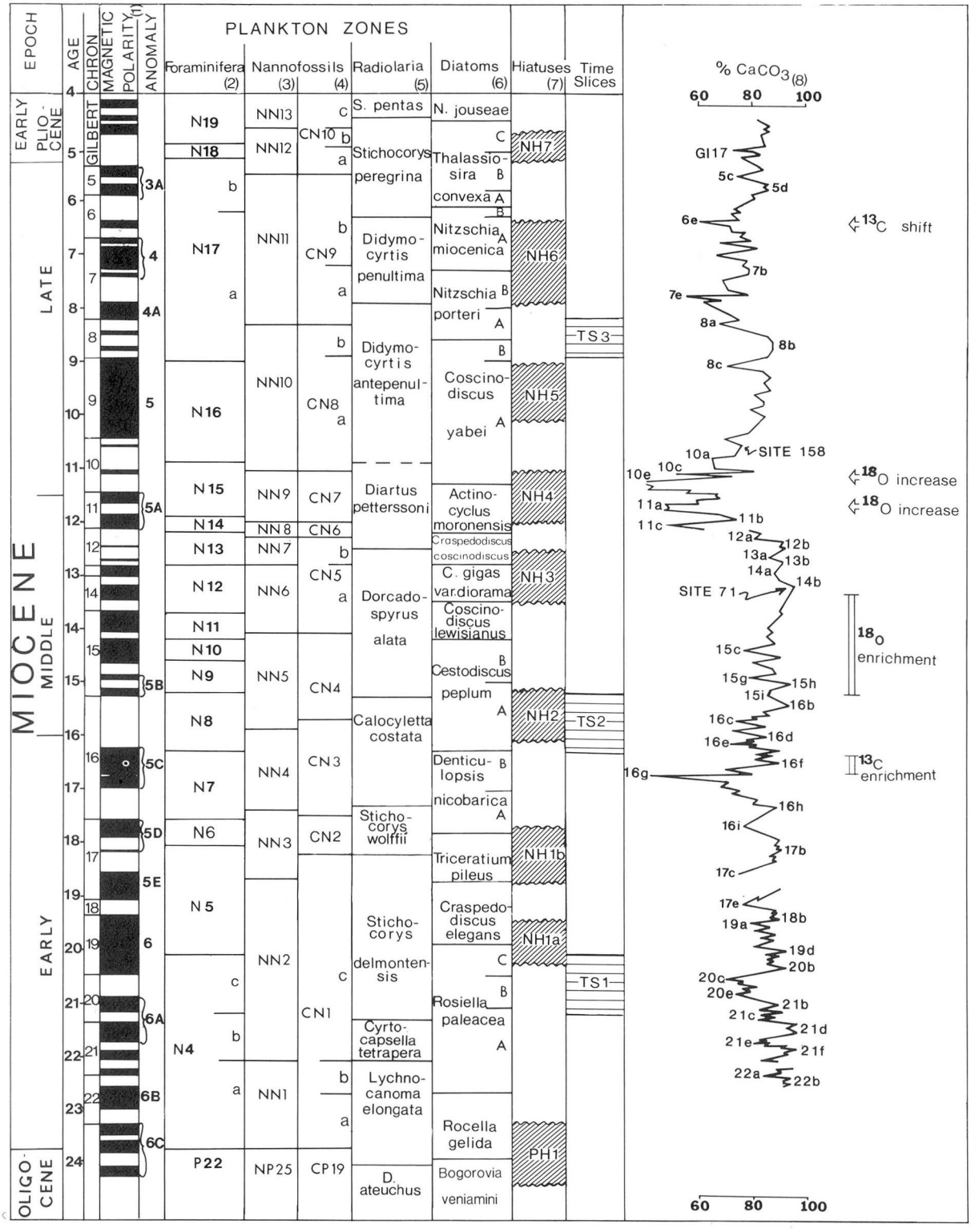

Figure 1. Correlation of planktonic microfossil zones, widespread deep sea hiatuses, the CENOP time slices, and the percent $CaCO_3$ curve for the eastern equatorial Pacific to the paleomagnetic time scale for the Miocene. (1) = Berggren et al., 1984; (2) = Blow, 1969; Srinivasan and Kennett, 1981a, b; Keller, in press; (3) = Martini, 1971; (4) = Bukry 1973, 1975; Okada and Bukry, 1980; (5) = Riedel and Sanfilippo, 1978; (6) = Burckle, 1972; Barron, 1983, in press; and (7) = Keller and Barron, 1983; (8) = Dunn and Moore, 1981; Dunn 1982.

of planktonic foraminiferal Zone N15, middle of calcareous nannofossil Zones NN9 and CN7, and near the first occurrence of the radiolarian *Didymocyrtis antepenultima* according to Berggren (1981) and Theyer et al. (1978). Ryan et al. (1974) place the boundary slightly lower at ~11.8 Ma.

Following Cita (1975) and Burckle (1978), the Miocene/-Pliocene boundary lies within the middle of the lower reversed event of the Gilbert paleomagnetic Chron at ~5.2 Ma. The Miocene/Pliocene boundary thus falls at the base of planktonic foraminiferal Zone N18, within calcareous nannofossil Zone NN12, in uppermost calcareous nannofossil Subzone CN10a, and near the Subzone A/Subzone B boundary of the *Thalassiosira convexa* Zone of diatoms.

At least five isotopic events are also useful for Miocene stratigraphy (Fig. 1 right side). The distinctive latest Miocene carbon shift (at 6.4 Ma on this time scale) involves an apparently permanent –0.5 ‰ depletion in $\delta^{13}C$ of the tests of benthic foraminifers and has been shown to be isochronous across the Pacific and Indian Oceans (Haq et al., 1980; Vincent et al., 1980). More recently, Vincent and Killingley (in press) have identified an isochronous +0.5 ‰ enrichment in the $\delta^{13}C$ of foraminifers which occurs in uppermost planktonic foraminiferal Zone N7 and is correlative with paleomagnetic Anomaly 5C in numerous cores in the Pacific and Indian Oceans.

The +1.0 ‰ increase in benthic foraminiferal $\delta^{18}O$ which occurs within planktonic foraminiferal zones N9 to lower N12 is widely recognizable throughout the ocean basins (Woodruff et al., 1981; Savin et al., 1981). Finally, Keigwin (1979) and Burckle et al. (1982) have shown that two distinctive oxygen isotope enrichment events occur in benthic foraminiferal tests across the middle Miocene/late Miocene boundary at DSDP Site 158. The first correlates with lower paleomagnetic Chron 11 (~11.7 Ma) and involves an increase of about +0.5 ‰ (11.3 Ma) in $\delta^{18}O$. The second correlates with lower paleomagnetic Chron 10 and involves an increase of ~ +0.7 ‰ in $\delta^{18}O$ (see also Keller et al., 1982).

Datum Events

Beyond the Miocene time scale shown in Figure 1, development of a high resolution Miocene chronostratigraphy should incorporate numerous additional microfossil datum levels within the individual zones and subzones which have been shown to be isochronous over widespread geographic areas. Many stratigraphically useful Miocene datum levels have been proposed for planktonic foraminifers (Keller, 1980a,b, 1981a,b; Srinivasan and Kennett, 1981a,b, Saito, 1977; Berggren et al., 1983), radiolarians (Theyer et al., 1978; Riedel and Sanfilippo, 1978), and diatoms (Burckle, 1978; Barron, in press). Direct correlation of planktonic foraminiferal (Saito et al., 1975; Poore et al., 1983), calcareous nannofossil (Gartner, 1973; Haq et al., 1980; Poore et al., 1983), radiolarian (Theyer et al., 1978; Johnson and Wick, 1982), and diatom (Burckle, 1978; Burckle et al., 1982) datum levels with paleomagnetic stratigraphy and graphical correlation plots (Shaw, 1964) provide the basis for testing the sequence and isochroneity of various microfossil datum events in different stratigraphic sections. Numerous age estimates can be assigned to the datum levels tied directly to paleomagnetic stratigraphy using the paleomagnetic polarity time scale of Berggren et al. (1984), and age versus depth plots can be constructed for individual stratigraphic sections in order to extrapolate the ages of additional datum levels (Barron, 1980; Keller, 1981b).

Tables 1–4 list stratigraphically important planktonic foraminiferal, calcareous nannofossil, radiolarian, and diatom datum levels for the Miocene and estimates of their ages according to the paleomagnetic time scales of Berggren et al. (1984) and Mankinen and Dalrymple (1979). An additional column lists the ages which result from utilizing an Anomaly 5-paleomagnetic Chron 11 correlation rather than the more traditional Anomaly 5-Chron 9 correlation. The basis for inclusion of this third column is discussed in the addendum. All discussion prior to the addendum utilizes the column 1 ages derived from the Berggren et al. (1984) paleomagnetic time scale and the traditional Anomaly 5-Chron 9 correlation and constitutes the adopted CENOP time scale.

Datum levels that have been tied directly to paleomagnetic stratigraphy are identified by an asterisk. Graphical correlation techniques were applied to over 20 DSDP sections in the Pacific (including DSDP Sites 71, 77, 158, 173, 289, 292, 470, and 495) in order to construct these tables. Microfossil data used in these compilations are predominantly from recent studies by CENOP workers (Keller, 1980a, b, 1981a, b; Keller et al., 1982; Srinivasan and Kennett, 1981a, b; Burckle et al., 1982; Barron, 1981a, b, 1983; Dunn, 1982). These data were supplemented by data published in the Initial Reports of the Deep Sea Drilling Project (Initial Reports): Volumes 7 (1971), 8 (1971), 9 (1972), 16 (1973), 17 (1973), 18 (1973), 30 (1975), 31 (1975), 32 (1975), 41 (1977), 63 (1982), and 67 (1982) as well as radiolarian data from Westberg and Riedel (1978). Tables 1–4 represent the composite of numerous graphical correlations which have incorporated 72 direct ties of microfossil datum levels to paleomagnetic stratigraphy between 24 and 4.3 Ma (10 planktonic foraminiferal, 9 calcareous nannofossil, 27 radiolarian, and 26 diatom).

Published correlations of additional datum levels to paleomagnetic stratigraphy have been discarded, because they were not consistent with graphical correlations (Keller et al., 1982). Correlation of a datum level to paleomagnetic stratigraphy in one core is no guarantee that the correlation is consistent (isochronous) with correlations elsewhere. For example, Theyer et al.'s (1978) correlation of the first appearance of the radiolarian *Diartus petterssoni* with paleomagnetic Chron 11 is rejected, because graphical correlations based on diatom and planktonic foraminiferal calibrations indicate that such a calibration date is too young. Similarly, Johnson and Wick (1982) show that many radiolarian datum levels vary as much as 0.6 m.y. in age in central equatorial Pacific cores for which the paleomagnetic stratigraphy has been measured.

Tables 1–4 are limited by the lack of total uniformity among

TABLE 1. AGES OF STRATIGRAPHICALLY-IMPORTANT MIOCENE PLANKTONIC FORAMINIFERAL DATUM LEVELS

Datum	Paleomag. Correl.	Age (Ma) "B84"	"MD79"	"B84!"
B. Sphaeroidinella dehiscens (z)	5th(-), Gilbert	4.9*(1)	4.9*	nc
B. Globorotalia tumida (z)	5th(-), Gilbert	5.2*(1)	5.1*	nc
T. Globoquadrina dehiscens (tropics)	5th(-), Gilbert	5.25*(1)	5.2*	nc
B. Globorotalia margaritae	(-), Chron 5	5.6*(1)	5.5*	nc
B. Pulleniatina primalis (sz)		6.3	6.1	nc
B. Globorotalia conomiozea	1st(-), Chron 6	6.3*(2, 3)	6.1*	nc
B. Globigerinides conglobatus		8.0	7.7	7.1
T. G. kennetti (temp.)		8.0	7.8	7.1
B. Neogloboquadrina pachyderma (temp.)		8.9	8.5	7.8
B. G. obliquus extremus		9.0	8.6	8.0
B. Globorotalia plesiotumida (z)		9.0	8.6	8.0
B. Globigerinoides kennetti (temp.)		10.1	9.7	8.1
T. Globoquadrina dehiscens (temp.)		10.3	9.9	8.2
B. G. merotumida		10.8	10.4	8.5
B. Neogloboquadrina acostaensis (z)	2nd(-), Chron 10	10.9*(2)	10.5*	8.6*
T. Globorotalia siakensis (z)		11.9	11.7	9.9
T. Globorotalia mayeri	low, Chron 11	11.9*(2	11.7*	9.9*
B. Globigerina nepenthes (z)		12.2	12.0	10.9
B. Globorotalia menardii		12.7	12.4	11.5
T. G. fohsi robusta		12.8	12.5	11.8
B. Sphaeroidinella subdehiscens (z)		12.8	12.5	11.8
B. S. seminulina		13.1	12.8	12.4
B. G. fohsi lobata		13.5	13.2	13.0
B. G. fohsi fohsi (z)		13.7	13.5	13.5
B. G. fohsi praefoshi (z)		14.2	14.0	14.0
T. G. archaeomenardii		14.5	14.3	nc
B. G. peripheroacuta (z)		14.6	14.4	nc
B. Orbulina suturalis (z)	lowest(+), Chron 15	15.2*(4)	15.1*	nc
T. Globigerinoides diminutus		15.6	15.5	nc
B. Globorotalia archaeomenardii		15.7	15.6	nc
B. Globigerinoides mitra		16.0	15.9	nc
B. G. sicanus (z)		16.4	16.3	nc
B. G. bisphaericus		16.4	16.3	nc
B. Globorotalia peripheroronda		16.5	16.4	nc
T. Catapsydrax stainforthi		16.7	16.7	nc
T. G. zealandica incognita		17.3	17.3	nc
T. C. dissimilis (z)	uppermost, Chron 17	17.6*(5)	17.6*	nc
B. Globigerinatella insueta (z)	1st(+), Chron 17	18.1*(5)	18.1*	nc
T. Globigerina binaiensis		18.2	18.2	nc
B. Globorotalia miozea		18.8	18.9	nc
B. G. praescitula		18.8	18.8	nc
T. G. acrostoma		19.7	19.8	nc
B. G. zealandica pseudomiozea		19.9	20.0	nc
T. G. kugleri (z)		20.1	20.3	nc
B. Dentoglobigerina altispira		20.7	20.9	nc
B. Globorotalia zealandica incognita		21.1	21.3	nc
T. G. mendacis		21.2	21.4	nc
B. Globoquadrina dehiscens (sz)		21.2	21.4	nc
B. Globorotalia acrostoma		21.7	21.9	nc
B. Globigerinoides trilobus immaturus (sz)		22.1	22.3	nc
B. Globorotalia kugleri (z)	2nd(+), Anomaly 6C	23.7*(6)	24.0*	nc

(z) = zonal marker; (sz) = subzonal marker; (temp.) = temperature datum. (-) = reversed polarity event; (+) = normal polarity event. * = direct paleomagnetic calibration. nc = no change.
Three age estimates are given based on three paleomagnetic time scales: "B84" = Berggren et al., 1984; "MD79" = Mankinen and Dalrymple, 1979; "B84!" = Berggren et al., 1984 using an Anomaly 5-Chron 11 correlation.
References: (1) = Saito et al., 1975; (2) = Ryan et al., 1974; (3) = Loutit and Kennett, 1979; (4) = Poore et al., 1983; (5) = Barron et al., in press; and (6) = Berggren et al., 1984.

TABLE 2. AGES OF STRATIGRAPHICALLY-IMPORTANT MIOCENE CALCAREOUS NANNOFOSSIL DATUM LEVELS

Datum	Paleomag. Correl.	Age (Ma) "B84"	"MD79"	"B84!"
B. Ceratolithus rugosus (sz) (z)	c_2 event, Gilbert	4.7*(1)	4.6*	nc
B. C. acutus (sz)	5th(-), Gilbert	5.0*(1)	5.0*	nc
T. Discoaster quinqueramus (z)	top of (-), Chron 5	5.5*(1)	5.4*	nc
B. Amaurolithus primus (sz)	base of (+), Chron 6	7.2#	7.0#	6.5*(2)
B. D. quinqueramus (z)	top of Chron 8†	8.3*(2)	8.0*	7.3*
B. D. neorctus (sz)		8.9	8.5	8.0
T. D. hamatus (z)	2nd (+), Chron 10	11.1*(3)	10.7*	8.8*
T. Catinaster coalitus		11.3	11.0	8.9
B. D. hamatus (z)		11.9	11.7	10.0
B. C. coalitus (z)		12.3	12.1	10.8
B. D. kugleri (sz)(z)		12.8	12.5	11.8
T. Sphenolithus heteromorphus (z)		14.0	13.9	nc
B. Calcidiscus macintyrei (z)		15.7	15.5	nc
B. D. exilis (z)	mid 1st(-), Chron 16	15.9*(4)	15.8*	nc
T. S. belemnos (z)		17.4	17.4	nc
B. S. heteromorphus (z)	lowermost Chron 16	17.5*(5)	17.5*	nc
B. S. belemnos (z)	2nd(-), Chron 17	18.2*(5)	18.2*	nc
T. Triquetrorhabdulus carinatus (z)	Anomaly 5E	18.7*(3)	18.7	nc
B. recurrent D. druggi		19.5	19.6	nc
B. D. druggii (sz)(z)		22.1	22.3	nc
T. abundant Cyclicargolithus abisectus (sz)		22.7	22.9	nc
T. Reticulofenestra bisecta	1st(+), Anomaly 6C	23.4*(4)	23.7*	nc
T. Sphenolithus ciperoensis (z)	2nd(+), Anomaly 6C	23.7*(4)	24.0*	nc

(z) = zonal marker; (sz) = subzonal marker. (+) = normal polarity event; (-) = reversed polarity event. * = direct paleomagnetic calibration. nc = no change.
Three age estimates are given based on three paleomagnetic time scales: "B84" = Berggren et al., 1984; "MD79" = Mankinen and Dalrymple, 1979; "B84!" = Berggren et al., 1984 using an Anomaly 5-Chron 11 correlation.
References: (1) = Gartner, 1973; (2) = Haq et al., 1980; (3) = Ryan et al., 1974; (4) = Poore et al., 1983; and (5) = Barron et al., in press.
= extrapolates to older age in traditional time scale (see Poore, 1981, and Keller et al., 1982).
† = correlates with lower Chron 7 (Anomaly 4) in alternate time scale.

micropaleontologists in recording the same datum levels in different cores. This is especially true for the radiolarians, where Theyer et al. (1978) and Johnson and Wick (1982) have proposed numerous datum levels that have not been recorded consistently by radiolarian workers in the Initial Reports or by Westberg and Riedel (1978). Similarly, although additional calcareous nannofossil datum levels for the Miocene have been proposed (Haq et al., 1980; Shafik, 1975), Bukry's papers in the Initial Reports typically only record his zonal and subzonal markers. In constructing Tables 1–4, we have found it preferable to use the data of as few as workers as possible for each microfossil group in order to lessen the effect of differing taxonomic concepts between workers. Planktonic foraminiferal data are mainly from the various papers of Keller and Srinivasan and Kennett, calcareous nannofossil data are derived mainly from the papers of Bukry in the Initial Reports, and diatom data are from the studies of Barron and Burckle. Radiolarian data, on the other hand, are drawn from the Initial Reports, Riedel and Sanfilippo (1978), and Dunn (1982). We acknowledge that differing taxonomic concepts by other micropaleontologists might lead to different age estimates for selected datum levels.

We have listed the datum levels which show the most consistency in the numerous cores that we have studied. We acknowledge that individual datum levels may have an imprecision of from 0.1–0.3 m.y. (Johnson and Wick, 1982), but have listed the most consistent age for each.

Sediment Accumulation Rate Curves

Sediment accumulation rate plots for the Miocene of DSDP Sites 71, 77, and 289 (Figures 2–4) show our interpretations of the record at these key sites and provide a means for assigning estimated ages to time series studies. These plots utilize the paleomagnetic time scale of Berggren et al. (1984) because it incorporates more chronological calibration points than the Mankinen and Dalrymple (1979) paleomagnetic time scale.

Site 71 generally has a good early and middle Miocene record (Fig. 2) which accumulated at relatively high (32 m/m.y.) rates. In the later part of the early Miocene (18.8–16.8 Ma) sediment accumulation rates are lower (8 m/m.y.), probably due to carbonate dissolution. However, a middle early Miocene hiatus (NH 1 b) proposed by Keller (1981b) is not apparent by the refined correlations of this paper. A hiatus occurs in the early late Miocene between 10.5 and 9.0 Ma (NH 5), and a second hiatus occurs across the Oligocene/Miocene boundary (Keller and Barron, 1983; Barron, 1983). Sediment accumulation rates in the

TABLE 3. AGES OF STRATIGRAPHICALLY-IMPORTENT MIOCENE RADIOLARIAN DATUM LEVELS

Datum	Paleomag. Correl.	Age (Ma) "B84"	"MD79"	"B84!"
T. Solenosphaera omnitubus	3rd(-), Gilbert	4.3*(1)	4.25*	nc
Spongaster berminghami→S. pentas (z)	c_1 event, Gilbert	4.45*(1)	4.4*	nc
B. Pterocanium prismatium	4th(+), Gilbert	4.6*(1)	4.5*	nc
T. Acrobotrys tritubus		5.5	5.4	nc
Stichocorys delmontensis→S. peregrina (z)	1st(-), Chron 6	6.3*(1)	6.1*	nc
B. Solenosphaera omnitubus		7.3	7.0	6.8
T. Diartus hughesi (z)		7.9	7.6	7.0
T. Didmocyrtis laticonus		8.9	8.5	7.5
B. A. tritubus		9.1	8.7	7.6
B. D. penultima		9.8†	9.5†	7.9*(1)
B. Spongaster berminghami		9.8	9.5	7.9
T. Stichocorys wolfii		10.4	10.0	8.2
T. Diartus petterssoni		10.4†	10.0†	8.2*(1)
D. petterssoni→D. hughesi (z)	2nd(-), Chron 10	10.9*(2)	10.3*	8.6*
B. D. hughesi	uppermost Chron 11	11.5*(1)	11.3*	9.0*
B. Didymocyrtis antepenultima	uppermost Chron 11	11.5*(1)	11.3*	9.0
T. Cyrtocapsella tetrapera	lower Chron 12	12.5*(2)	12.2*	11.4*
T. C. cornuta		12.5	12.2	11.4
B. Diartus petterssoni (z)	lower Chron 12	12.6*(2)	12.3*	11.5*
B. Didymocyrtis laticonus	uppermost Chron 15	13.8*(1)	13.6*	nc
B. Lithopera neotera	2nd(-), Chron 15	14.5*(1)	14.3*	nc
T. Calocyletta costata	upper (+), Anom. 5A	14.9*(1)	14.6*	nc
Dorcadospyris dentata→D. alata (z)		15.3	15.2	nc
B. D. alata	uppermost Chron 16	15.5*(1)	15.4*	nc
T. Didymocyrtis prismatica		15.8	15.7	nc
T. Lychnocanoma elongata		15.9	15.8	nc
B. Calocyletta costata (z)	lower Chron 16	17.3*(3)	17.3*	nc
B. Dorcadospyris dentata	lower Chron 16	17.3*(3)	17.3*	nc
B. Stichocorys wolfii	2nd (-), Chron 17	18.2*(3)	18.2*	nc
B. Lirospyris stauropora		18.4	18.4	nc
T. Calocyletta serrata		19.2	19.3	nc
B. Dorcadospyris forcipata		19.6	19.7	nc
T. D. ateuchus	upper Chron 19	19.7*(1)	19.8*	nc
T. Cyclamterium pegetrum	upper Chron 19	19.8*(1)	19.9*	nc
T. C. leptetrum		20.0	20.1	nc
B. Didymocyrtis violina	lower Chron 19	20.2*(1)	20.3	nc
B. D. tubaria		20.3	20.4	nc
B. Stichocorys delmontensis	(+), Chron 20	21.1*(1)	21.3*	nc
T. Theocyrtis annosa (z)	lowermost Chron 20	21.3*(1)	21.5*	nc
B. Calocyletta virginis	uppermost Chron 21	21.5*(1)	21.7*	nc
B. C. serrata	1st (+), Chron 21	21.7*(1)	21.9*	nc
B. Cyrtocapsella cornuta		22.1	22.3	nc
B. C. tetrapera (z)		22.1	22.3	nc
T. Dorcadospyris papillio		22.6	22.8	nc
T. Artophormis gracilis		22.6	22.8	nc
B. Lychnocanoma elongata (z)		24.1	24.3	nc

(z) = zonal marker. (-) = reversed polarity event; (+) = normal polarity event.
* = direct paleomagnetic calibration. † = these datums extrapolate to older relative ages under the traditional time scale (Fig. 1). nc = no change.
Three age estimates are given based on three paleomagnetic time scales: "B84" = Berggren et al., 1984; "MD79" = Mankinen and Dalrymple, 1979; "B84!" = Berggren et al., 1984, using an Anomaly 5-Chron 11 correlation.
References: (1) = Theyer et al., 1978; (2) = Johnson and Wick, 1982; (3) Barron et al., in press.

proximity of the middle Miocene/late Miocene boundary (12.5–10.5 Ma) are 16 m/m.y., whereas most of the upper Miocene (9.0–5.4 Ma) accumulated at a lower (9 m/m.y.) rate.

The record at Site 77 (Fig. 3) resembles that at Site 71 in that it contains an early late Miocene (10.5–9.0 Ma) (NH 5) hiatus. Two early Miocene hiatuses (20.3–19.8 Ma = NH 1a and 19.0–17.8 Ma = NH 1b), however, are also present at Site 77 (Keller, 1980a; Keller and Barron, 1983). The early Miocene interval between about 23.6 and 20.3 Ma accumulated at a rate of 18 m/m.y. Similarly, most of the middle and late Miocene accumulated at a rate of 14 m/m.y., with the exception of a brief interval (13.5–12.0 Ma) which accumulated at a rate of 20 m/m.y. The near vertical drop in the Site 77 plot at about 6 Ma corresponds with Core 77B-11 where only 1.5 m of sediment was recovered in a standard 9.5 m-long core barrel. An abrupt, short-term increase in the sediment accumulation rates between 100

TABLE 4. AGES OF STRATIGRAPHICALLY-IMPORTANT MIOCENE DIATOM DATUM LEVELS

Datum	Paleomag. Correl.	Age (Ma) "B84"	"MD79"	"B84!"
B. Nitzschia jouseae (z)	3rd (-), Gilbert	4.5*(1)	4.45*	nc
T. Thalassiosira miocenica (sz)	4th (-), Gilbert	5.1*(1)	5.0*	nc
B. T. oestrupii	4th (-), Gilbert	5.1*(1)	5.0*	nc
T. Asterolampra acutiloba	top Chron 5	5.35*(1)	5.25*	nc
T. N. miocenica	mid (-), Chron 5	5.6*(1)	5.5*	nc
T. T. praeconvexa (sz)	lower Chron 5	5.8*(1)	5.7*	nc
B. T. convexa var. aspinosa (z)	upper Chron 6	6.1*(1)	6.0*	nc
B. T. miocenica	upper Chron 6	6.15*(1)	6.05*	nc
B. T. praeconvexa (sz)	1st (-), Chron 6	6.3*(1)	6.2*	nc
B. Denticulopsis kamtschatica (z) (temp.)	2nd (-), Chron 6	6.6*(2)	6.4*	nc
T. N. porteri	upper Chron 7	7.2*(1)	7.0*	6.7*
B. N. miocenica (z)	upper Chron 7	7.3*(1)	7.1*	6.8*
T. Rossiella paleacea	middle Chron 7	7.4*(1)	7.2*	6.9*
T. Thalassiosira burckliana (sz)	lower Chron 7	8.0*(1)	7.7*	7.0*
T. Coscinodiscus yabei (z)	middle Chron 8	8.6*(1)	8.3*	7.5*
B. T. antiqua (temp.)		8.7	8.4	7.6
B. T. burcklina (sz)	uppermost Chron 9	9.0*(1)	8.7*	8.0*
T. C. temperei var. delicata		9.8	9.5	8.2
T. Denticulopsis dimorpha (temp.)		10.5	10.1	8.6
T. C. vetustissimus var. javanica	upper Chron 10	10.7*(1)	10.3*	8.5
B. C. vetustissimus var. javanica	lower Chron 10	11.2*(1)	10.8*	8.8*
T. Actinocyclus moronensis(z)	lower Chron 10	11.3*(1)	11.0*	8.9*
B. D. dimorpha (temp.)		11.3	11.0	8.9
T. C. tuberculatus	lowermost Chron 12	12.0*(3)	11.7*	10.4*
T. D. punctata f. hustedtii	uppermost Chron 12	12.2*(3)	11.9*	10.7*
T. Craspedodiscus coscinodiscus (z)		12.2	11.9	10.7
B. Hemidiscus cuneiformis	middle Chron 12	12.6*(1)	12.4*	11.2*
B. Rhizosolenia barboi (temp.)		12.6	12.4	11.2
B. C. temperei var. delicata (z)	lowermost Chron 12	12.8*(3)	12.6*	11.8
T. Denticulopsis nicobarica		13.2	13.0	12.6
B. D. praedimorpha (temp.)		13.4	13.3	12.9
T. C. lewisianus (z)		13.5	13.4	12.9
B. D. hustedtii (tropics)		13.7	13.6	nc
T. Cestodiscus peplum (z)	1st (-), Chron 15	14.1*(1)	14.0*	nc
B. D. hyalina (temp.)		15.0	14.9	nc
T. Annellus californicus (sz)	3rd (-), Chron 15	15.0*(1)	14.9*	nc
B. Actinocyclus ingens (tropics)		15.5	15.4	nc
B. D. lauta (temp.)		16.1	16.0	nc
B. Cestodiscus peplum (z)	upper Anomaly 5C	16.4*(4)	16.3*	nc
T. Thalassiosira fraga		16.4	16.3	nc
T. T. bukryi (sz)	lower Chron 16	17.0*(4)	17.1*	nc
B. D. nicobarica (z)	1st (+), Chron 17	17.8*(4)	17.8*	nc
T. Actinocyclus radioovae	1st (-), Chron 17	18.0*(4)	18.9*	nc
T. Craspedodiscus elegans (z)		18.7	18.8	nc
B. Nitzschia maleinterpretaria		18.8	18.9	nc
T. Bogorovia veniamini (z)	Chron 19	19.9*(2)	20.0*	nc
B. T. fraga		19.9	20.0	nc
T. Coscinodiscus oligocenicus (sz)		20.6	20.7	nc
B. A. radionovae		21.2	21.4	nc
T. T. primalabiata (sz)		21.7	21.9	nc
B. Craspedodiscus elegans		22.2	22.4	nc
T. Coscinodiscus lewisianus var. rhomboides		22.5	22.8	nc
B. Rossiella paleacea (z)		22.7	23.0	nc
T. Rocella gelida s. ampl.		22.7	23.0	nc
B. R. gelida var. schraderi		23.6	23.9	nc
B. R. gelida s. str.		24.0	24.3	nc

(z) = zonal marker; (sz) = subzonal marker; (temp.) = temperate datum. (-) = reversed polarity event; (+) = normal polarity event. * = direct paleomagnetic calibration. nc = no change. Three age estimates are given based on three paleomagnetic time scales: "B84" = Berggren et al., 1984; "MD79" = mankinen and Dalrymple, 1979; "B84!" = Berggren et al., 1984, using an Anomaly 5-Chron 11 correlation.

References: (1) = Burckle, 1978; (2) = Burckle, oral comm., 1982; (3) = Burckle et al., 1982; and (4) = Barron et al., in press.

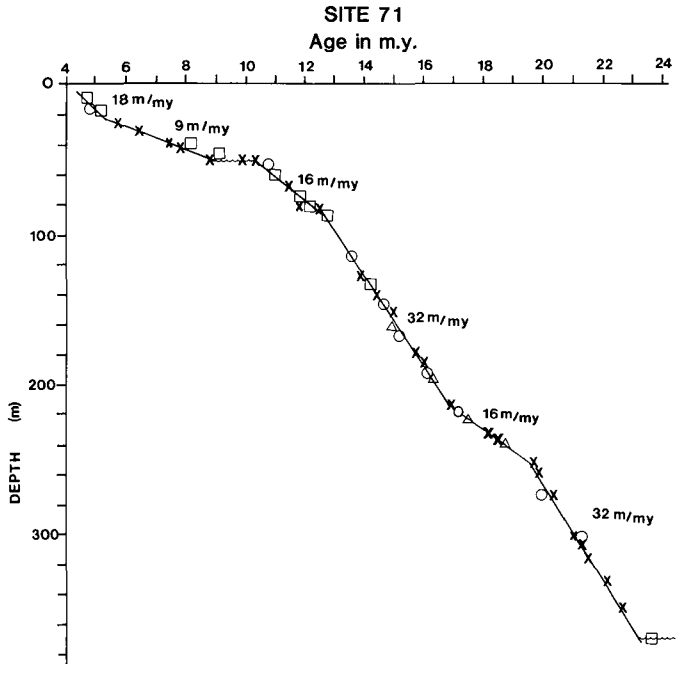

Figure 2. Sediment accumulation rate plot of the Miocene of DSDP Site 71. ○ = planktonic foraminiferal datum; □ = calcareous nannofossil datum; X = radiolarian datum; Δ = diatom datum. Refer to Tables 1–4 for age of datums.

and 110 m subbottom depth in Hole 77B has been plotted on Figure 3, but the results at DSDP Site 573 (Barron et al., in press), only 10 km from Site 77, do not reveal such an abrupt change in sediment accumulation rates there.

Site 289 has the most complete Miocene section of the three sections with only a short hiatus at 12.0–11.5 Ma (NH 4) (Keller, this volume) (Fig. 4). Hiatus NH 1 of Keller and Barron (1983) (~18.0–17.5 Ma) has been discounted at Site 289 by refinements in biostratigraphy. However, reduced sediment accumulation rates (20 m/m.y.) also characterize the late early Miocene (18.7–16.3 Ma) and late Miocene (10.9–6.4 Ma) at Site 289 within intervals which either contain hiatuses, or exhibit similarly reduced sedimentation rates as at Sites 71 and 77 (Figs. 2, 3). Higher accumulation rates (50 m/m.y.) characterize the upper part of the middle Miocene (14.0–12.0 Ma) and the latest part of the Miocene (6.4–5.1 Ma). Moderate rates correspond with the earliest Miocene (37 m/m.y. between 23.7 and 18.7 Ma) and the early middle Miocene (30 m/m.y. between 16.3 and 14.0 Ma). Site 289 on the Ontong-Java Plateau (2206 m water depth) apparently was above most of the erosive and corrosive effects of bottom waters which caused most of the deep-sea hiatuses of the Miocene (Keller and Barron, 1983). Comparison of the Site 289 sediment accumulation rate plot (Fig. 4) with the generalized carbonate curve for the Miocene (Fig. 1), however, shows a strong correspondence between intervals of lower accumulation rates and intervals of lower average percent carbonate values (18.7–15.3 Ma and 12.0–6.4 Ma). Presumably, this correspondence reflects greater carbonate dissolution during those intervals.

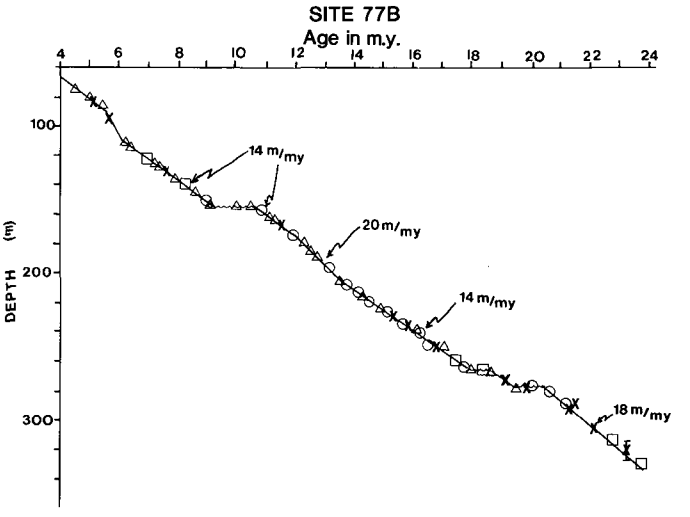

Figure 3. Sediment accumulation rate plot of the Miocene of DSDP Site 77. See Fig. 2 caption for explanation of the symbols.

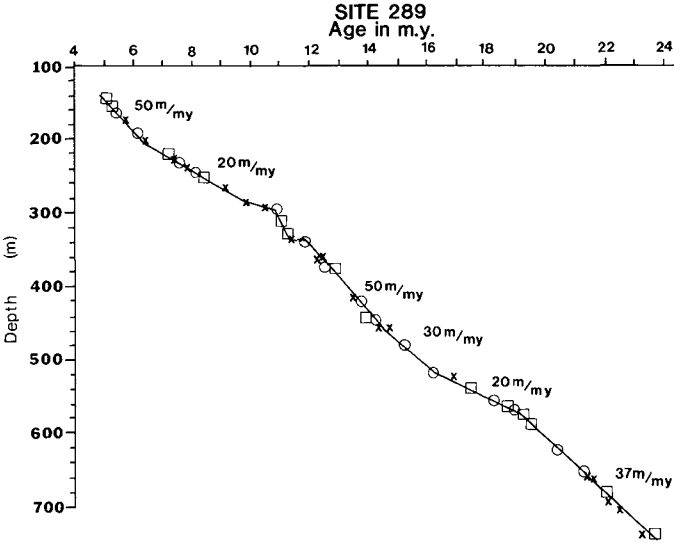

Figure 4. Sediment accumulation rate plot of the Miocene of DSDP Site 289. See Fig. 2 caption for explanation of the symbols.

TIME SLICE INTERVALS

The early, middle, and late Miocene are each marked by major paleoclimatic and paleoceanographic events which fundamentally changed the oceanic regime as expressed by the oxygen and carbon isotope records (Woodruff et al., 1981; Savin et al., 1981) and by changing faunal and floral assemblages (Haq, 1980; Kennett, 1977; Keller and Barron, 1983). CENOP workers chose three time-slice intervals for detailed study close to the major Miocene paleoceanographic events in order to characterize the evolving Miocene ocean as well as faunal and floral responses. Each time-slice interval spans between 0.5 and 1 m.y., and uncertainties of correlation are minimized by study of multiple samples from each of the time-slice intervals in the various stratigraphic

sections. At the same time, because correlations between middle and low latitudes typically have an uncertainty of at least 0.5 m.y., choice of 0.5–1 m.y.-long time slices allows a greater geographic coverage of the ocean basins. The three time slices near the beginning, the middle, and end of the Miocene provide a time lapse view of the history of the Miocene ocean.

Selecting time-slice intervals for study is difficult, primarily due to incomplete sedimentary records and imprecise biostratigraphic data and correlations. A prerequisite to choosing a time-slice interval should be that the interval be represented in as many stratigraphic sections (or DSDP holes) as possible. Certain limitations, such as the lack of a stratigraphic section in a given geographic region or the lack of recovery of a given stratigraphic interval, are unavoidable. Recognition of widespread deep sea hiatuses, which remove a specific interval from broad areas of the ocean basins, must be considered in selecting time slice intervals. Keller and Barron's (1983) study of Miocene deep sea hiatuses identified nine intervals of widespread hiatuses (Fig. 1) between the latest Oligocene and the Miocene/Pliocene boundary: 24.4–23.2 Ma (PH), 20.2–19.4 Ma (NH 1a), 18.7–17.7 Ma (NH 1b), 16.1–15.1 Ma (NH 2), 13.5–12.5 Ma (NH 3), 12.0–11.0 Ma (NH 4), 10.1–9.5 Ma (NH 5), 7.9–6.4 Ma (NH 6), and 5.2–4.7 Ma (NH 7) (Ages adjusted to the revised time scale of Fig. 1). Of these hiatuses, all except NH 2 are widespread in the Pacific and have been avoided in selecting Miocene time slices for study.

Climatically-warm intervals tend to be better represented in deep sea sequences than climatically-cool intervals which tend to correspond with widespread deep sea hiatuses (Barron and Keller, 1982). In addition, low-latitude microfossil zonations are recognizable over broader geographic regions during climatically-warm intervals than during climatically-cool intervals, and problems of correlation across latitudes are minimized. Consequently, climatically-warm intervals are better candidates for time-slice intervals than climatically-cool intervals.

The Miocene is a time of considerable paleoclimatic and paleoceanographic fluctuation (Savin et al., 1981; Haq, 1980; Barron and Keller, 1983; Keller, this volume), and ideally, time-slice intervals should be of minimal duration. The multidisciplinary time scale (Tables 1–4; Figure 1) developed here allows resolution of Miocene time approaching 100,000 years. Miocene correlations between tropical and temperate regions have been greatly improved in recent years (Keller and Barron, 1981; Keller et al., 1982; Srinivasan and Kennett, 1981b) and allow resolution of time of between 200,000 to 500,000-year range. In order to construct time slice maps that cover both high- and low-latitude areas of the oceans (the Pacific in particular), time-slice intervals of approximately 500,000 to one-million-years duration have been chosen for study. This alleviates many problems of nonrecovery of a time-slice interval and uncertainty of correlation. Undoubtedly, such lengthy intervals contain climatic fluctuations; however, an effort has been made to select generally warm and climatically-stable intervals. In addition, four or more samples per interval have been counted (measured) and averaged so as to reduce the effects of climatic fluctuation.

Early Miocene Time Slice (~21 Ma)-TS-1

The oldest time slice (~21 Ma) was chosen to characterize the early Miocene ocean prior to the major faunal turnover in planktonic foraminifers which is marked by a sharp decline and eventual extinction of Oligocene taxa and the rise of Neogene taxa (Keller, 1981a,b). The early Miocene time slice corresponds with Keller's (this volume) Subzone c of planktonic foraminiferal Zone N4, and precedes the widespread middle early Miocene deep sea hiatuses (20.2–19.4 Ma (NH 1a) and 18.7–17.7 Ma (NH 1b) (Keller, 1981b). As such, the base of the early Miocene time slice is defined by the first occurrence of *Globoquadrina dehiscens* and its top coincides with the last occurrence of *Globoquadrina kugleri* (Table 1). The early Miocene time slice also correlates with part of Martini's (1971) NN 2 Zone and with part of Subzone CN1c of Okada and Bukry (1980) (Figure 1). The base of the time slice corresponds with the last occurrence of the radiolarian *Theocyrtis annosa,* and its top is closely approximated by the first occurrence of *Didmocyrtis violina.* Consequently, the early Miocene time slice is equivalent to the lower part of the *Stichocorys delmontensis* Zone of Riedel and Sanfilippo (1978). In terms of diatoms, the time slice roughly corresponds with Subzones B and C of the *Rossiella paleacea* Zone of Barron (1983). The last occurrence of the diatom *Thalassiosira primalabiata* falls near the base of the time slice, and the last occurrence of *Bogorovia veniamini* slightly post-dates the top of the time slice. These two diatom datum levels are also recognizable in the high-latitude South Atlantic (Gombos and Ciesielski, 1983) and suggest that the early Miocene time slice (TS-1) should be recognizable in the Southern Ocean.

A distinctive carbonate dissolution interval (events 20c–20e of Dunn, 1982) characterizes the middle part of the early Miocene time slice with higher carbonate values lying at the top (events 20b–19e) and bottom (events 21c–21b) of the time slice.

Late Early Miocene Time Slice (~16 Ma)-TS-2

The major oxygen isotope event of the Miocene is the enrichment in δO^{18} by about 1.0 ‰ (cooling) which is recorded in benthic foraminifers during the early middle Miocene (planktonic foraminiferal zones N9 to N12) (Shackleton and Kennett, 1975; Woodruff et al., 1981; Savin et al., 1981). This globally recognized event has usually been interpreted as reflecting major increase in the size of the Antarctic ice sheet (Shackleton and Kennett, 1975; Woodruff et al., 1981; Savin et al., 1981) or major cooling (Matthews and Poore, 1980). The second Miocene time slice was chosen within planktonic foraminiferal Zone N8 across the early Miocene/middle Miocene boundary after the major planktonic foraminiferal faunal turnover in the middle early Miocene (Keller, 1981a) and prior to this major oxygen isotope event. It will be referred to as the late early Miocene time slice (TS-2). The base of this time slice is, therefore, defined by the first occurrence of *Globigerinoides sicanus* (16.4 Ma, Table 1) and the top by the first occurrence of *Orbulina suturalis* (15.2

Ma, Table 1). In terms of calcareous nannofossils, the late early Miocene time slice corresponds with the upper part of Zone NN4 to lower Zone NN5 of Martini (1971) and the upper part of Zone CN3 to lower part of Zone CN4 of Okada and Bukry (1980). The upper part of the *Calocyletta costata* Zone (radiolarians) of Riedel and Sanfilippo (1978) and nearly all of Subzone A of the *Cestodiscus peplum* Zone (diatoms) of Barron are also equivalent to the middle Miocene time slice.

In identifying the late early Miocene time slice it is necessary to consider the biostratigraphic data of two or more microfossil groups. Planktonic foraminiferal Zone N8 is difficult to recognize in the central and eastern equatorial Pacific, because its primary markers, *Globigerinoides sicanus* and *Orbulina suturalis,* are susceptible to dissolution (Jenkins and Orr, 1972; Keller, 1980b). Keller (1980b) suggests that the first occurrence of the resistant species *Globorotalia peripheroronda* (16.5 Ma) represents more reliable datum plane for approximating the base of Zone N8 in faunas affected by dissolution. Although Keller (1980b) also argues that the first occurrence of *G. archaeomenardii* is a secondary marker for the lower part of Zone N9, Table 1 shows that this datum (15.7 Ma) predates the *Orbulina* datum (15.2 Ma) (= base of Zone N9) by 0.5 m.y. Similarly, Bukry (1981) points out that the calcareous nannofossil *Helicosphaera ampliaperta* is sparse in deep-sea sediment, and that secondary criteria (i.e., the first occurrence of *Calcidiscus macintyrei*) had to be selected for recognition of the base of the *S. heteromorphus* Zone (CN4).

In the southwestern Pacific the time slice correlates with the uppermost part of the *Globorotalia miozea* Zone and the entire *Praeorbulina glomerosa* Zone (planktonic foraminifers) of Srinivasan and Kennett (1981b). In the middle-to-high latitude North Pacific, Subzone a of the *Denticulopsis lauta* Zone (diatoms) of Barron (1980) is equivalent to the time slice.

In the North Atlantic Ocean and Caribbean Sea, the interval of the late early Miocene time slice typically coincides with a hiatus (NH-2 of Keller and Barron, 1983). In the Pacific, however, hiatuses are relatively rare during this interval (Keller and Barron, 1983).

General carbonate dissolution (event 16e to 16c of Dunn 1982) characterizes the lower part of the early Miocene/middle Miocene time slice, whereas higher carbonate values (events 16b–15i) mark its top.

Late Miocene Time Slice (~8 Ma) -TS-3

The middle late Miocene interval correlative with paleomagnetic Chron 8 is the best represented late Miocene interval in deep-sea sections (Keller and Barron, 1983). Thus, this interval (8.9–8.2 Ma, according to the paleomagnetic time scale of Berggren et al., 1984) was chosen to characterize the late Miocene ocean after the middle Miocene oxygen isotope event and prior to the latest Miocene $\delta^{13}C$ (carbon) shift. The late Miocene time slice is equivalent to the lowermost part of planktonic foraminiferal Zone N17, the upper part of calcareous nannofossil Zone NN10 of Martini (1971), Subzone CN8b (calcareous nannofossil) of Okada and Bukry (1980), the upper part of the *Didmocyrtis antepenultima* Zone (radiolarians) of Riedel and Sanfilippo (1978), and Subzone B of the *Coscinodiscus yabei* Zone to lower Subzone A of the *Nitzschia porteri* Zone (diatoms) of Burckle (1972) and Barron (in press) (Fig. 1). The first occurrences of the planktonic foraminifer *Globorotalia plesiotumida* (9.0 Ma, Table 1), the calcareous nannofossil *Discoaster neorectus* (8.9 Ma), the radiolarian *Acrobotrys tritubus* (9.1 Ma), and the diatom *Thalassiosira burckliana* (9.0 Ma) closely approximate the base of the late Miocene time slice at low latitudes. The top of the time slice is immediately below the first occurrence of *Globigerinoides conglobatus* (planktonic foraminifer) (8.0 Ma) and the last occurrences of *Diartus hughesi* (radiolarian) (7.9 Ma) and *Thalassiosira burckliana* (diatom) (8.0 Ma).

There are considerable problems with placement of the N16/N17 planktonic foraminiferal zone boundary. The base of N17, the first occurrence of *Globorotalia plesiotumida,* is not only diachronous between low and middle latitudes (Keller, 1980a, 1981b), but it appears to be diachronous across the equatorial Pacific. In the eastern equatorial Pacific, the *G. plesiotumida* datum correlates with the upper part of paleomagnetic Chron 9 (~9.0 Ma) (Keller, 1981b; Keller et al., 1982), whereas in the western equatorial Pacific that datum correlates with the paleomagnetic Chron 7 (~7–8 Ma) (Srinivasan and Kennett, 1981a, b; Keller et al., 1982). Keller (this volume) suggests that an abundance peak in *G. menardii* at about 8 Ma can be used secondarily to locate the late Miocene time slice in low-latitude sections. In the middle-latitude North Pacific the late Miocene time slice corresponds closely with the range of *Globigerinoides kennetti* (planktonic foraminifer) (Keller, 1980a) and can also be recognized by the range of *Thalassiosira burckliana* (diatom) which appears to be isochronous within low latitudes (Barron, 1980, 1981a). Relatively high carbonate values (events 8d–8b of Dunn and Moore, 1981) characterize most of the late Miocene time slice, although a marked decline in carbonate values (event 8a) begins near the top of time slice TS-3.

SUMMARY

Integration of planktonic foraminiferal, calcareous nannofossil, radiolarian, and diatom datum levels in over 20 DSDP sections has resulted in a high resolution multiple microfossil biochronology for the Miocene. Direct correlations of over 70 datum levels to paleomagnetic stratigraphy and graphical correlations allow assignment of extrapolated absolute ages to 175 datum levels between 24.0 and 4.3 Ma (Tables 1–4). The resulting resolution of time approaches 100,000 years and is enhanced considerably by integration of carbonate stratigraphy (Dunn and Moore, 1981).

A Miocene time scale correlated with the paleomagnetic time scale of Berggren et al. (1984) is presented (Fig. 1). The main differences with previously published time scales are in the early Miocene where recent paleomagnetic correlations (Poore et al., 1983; Barron et al., in press) have resulted in changes. Specifi-

cally, the N4/N5 planktonic foraminiferal zonal boundary is correlated with the middle part of paleomagnetic Chron 19 (20.1 Ma), 0.5–2.0 m.y. younger than previous correlations Ryan et al., 1974; Saito, 1977; Keller, 1980a; Berggren, 1981; Srinivasan and Kennett, 1981a; Berggren et al., 1983).

Sediment accumulation rate curves are presented for key Miocene reference sections; DSDP Sites 71 and 77B in the eastern equatorial Pacific (Figs. 2, 3) and Site 289 in the western equatorial Pacific (Fig. 4). Sites 71 and 77B contain hiatuses in the early late Miocene (Keller and Barron, 1983), but Site 289 appears to have a nearly complete Miocene section. The middle early Miocene hiatus (~18.0–17.5 Ma) of Keller and Barron (1983) at Site 289 is discounted by refined correlations. Comparison of the Site 289 sediment accumulation rate plot (Fig. 4) with the generalized carbonate curve (Fig. 1) for the Miocene shows a strong correspondence between intervals of lower accumulation rates and lower percentage carbonate values (18.7–16.3 Ma and 12.0–6.4 Ma), most likely reflecting carbonate dissolution.

The three CENOP time slices (TS-1 at 21 Ma, TS-2 at 16 Ma, and TS-3 at 8 Ma) were chosen to avoid intervals of widespread deep-sea hiatuses (Keller and Barron, 1983) and to characterize the Miocene ocean immediately prior to three major paleoceanographic/paleoecologic events: the major faunal turnover of planktonic foraminifers in the middle early Miocene (Keller, 1981a, b), the major positive $\delta^{18}O$ increase (cooling) in benthic foraminifers during planktonic foraminifer Zones N9 to lower N12 (Woodruff et al., 1981), and the carbon shift (Haq et al., 1980; Vincent et al., 1980).

The early Miocene time slice corresponds with Keller's (in press) Subzone c of planktonic foraminiferal Zone N4 (21.2–20.1 Ma; given as 22 Ma in this volume). The late early Miocene time slice is defined by planktonic foraminiferal Zone N8 (16.4–15.2 Ma). The late Miocene time slice is equivalent to paleomagnetic Chron 8 (8.9–8.2 Ma) near the N16/N17 planktonic foraminiferal zone boundary.

ADDENDUM: ALTERNATE TIME SCALE

The time scale proposed in this paper and used throughout this volume incorporates a correlation of paleomagnetic Anomaly 5 with paleomagnetic Chron 9, a correlation which has been widely accepted for more than 10 years (Berggren and Van Couvering, 1974; Theyer and Hammond, 1974; Ryan et al., 1974). Recently, however, W. A. Berggren (oral comm., 1984) has suggested that Anomaly 5 should be correlated with Chron 11 (as it has been recognized in the sediment) based on paleomagnetic-biostratigraphic correlations at DSDP Site 519 in the South Atlantic by Poore et al. (1984) and Hsu et al. (1984). Site 519 was drilled on crust slightly older than Anomaly 5, and middle Miocene calcareous nannofossils (Zones NN8 and NN9) were recorded within a relatively long normally polarized interval (10 m) immediately above the basement (Poore et al., 1984). As correlations of NN8 and NN9 (=CN6 and CN7) calcareous nannofossils with paleomagnetic Chron 11 have been well established (Ryan et al., 1974; Berggren and Van Couvering, 1978; Keller et al., 1982), it seems apparent that the normally polarized interval containing NN8 and NN9 calcareous nannofossils at Site 519 correlates with both Anomaly 5 and Chron 11 (Hsu et al., 1984).

If one accepts an Anomaly 5-Chron 11 correlation, one must utilize an age assignment of 8.92–10.42 Ma for Chron 11 under the Berggren et al. (1984) paleomagnetic time scale. The middle Miocene/late Miocene boundary which is correlated with upper Chron 11 (Fig. 1) would then have an approximate age of 9.5 Ma. The paleomagnetic chrons above and below Chron 11 would also have to be correlated to the anomalies in a new manner (Theyer and Hammond, 1974). W. A. Berggren (oral comm., 1984) believes that the traditional correlations of chrons and anomalies (Ryan et al., 1974; LaBrecque et al., 1977; Fig. 1 of this report) above Chron 7 and below Chron 14 do not require adjustment. On Figure 5, a correlation used by Barron et al. (in press), which is basically that proposed by Theyer and Hammond (1974), is presented. The resultant polarity sequence in chrons 7 through 14 is similar to that in the more traditional time scales (Fig. 1), although Chron 7 is shortened to include only Anomaly 4 (3 normally polarized events) and Chron 14 is lengthened to include three additional normally polarized events below Anomaly 5A.

Tauxe et al. (1983) have proposed a system for labelling paleomagnetic chrons which is straightforward and avoids the nomenclatural problems with anomaly-chron correlations. Tauxe et al. (1983) label successive chrons from the top of one numbered anomaly to the top of the next oldest anomaly with the same number as the included anomaly and preface those numbers with a "C." Thus, Chron C5 includes Anomaly 5 plus the interval below Anomaly 5 and above Anomaly 5A (Fig. 5). However, most published paleomagnetic correlations of microfossil datum levels and virtually all of the papers of this volume refer exclusively to the older system of numbering chrons, so it is important to acknowledge it.

The alternate Miocene time scale utilizing an Anomaly 5-Chron 11 correlation is shown in Figure 5. The correlation of the microfossil zones and subzones with the paleomagnetic chrons on Figure 5 differs little from the correlation shown on Figure 1, but the estimated ages of zones and subzones between 6.5 and 13.8 (paleomagnetic Chrons 7–14) have been changed (compare Figs. 1 and 5). This correlation has been accomplished by reassigning ages to those microfossil datums correlated with Chrons 7 through 14 (see Tables 1–4) based on the anomaly-chron correlation model of Figure 5. Ages of additional datum levels (and zonal boundaries) have been extrapolated from replotted sediment accumulation rate plots (between 16 and 6 Ma) for Sites 71, 77, and 289 (Fig. 6) and from the sediment accumulation rate plots of Barron et al. (in press) for central Pacific DSDP Sites 572–574, which utilize the same time scale.

As a result of these changes, the estimated age of the late Miocene time slice (TS-3) becomes 8.0–7.0 Ma. Hiatuses NH 6 through NH 3 of Keller and Barron (1983) have recalculated ages

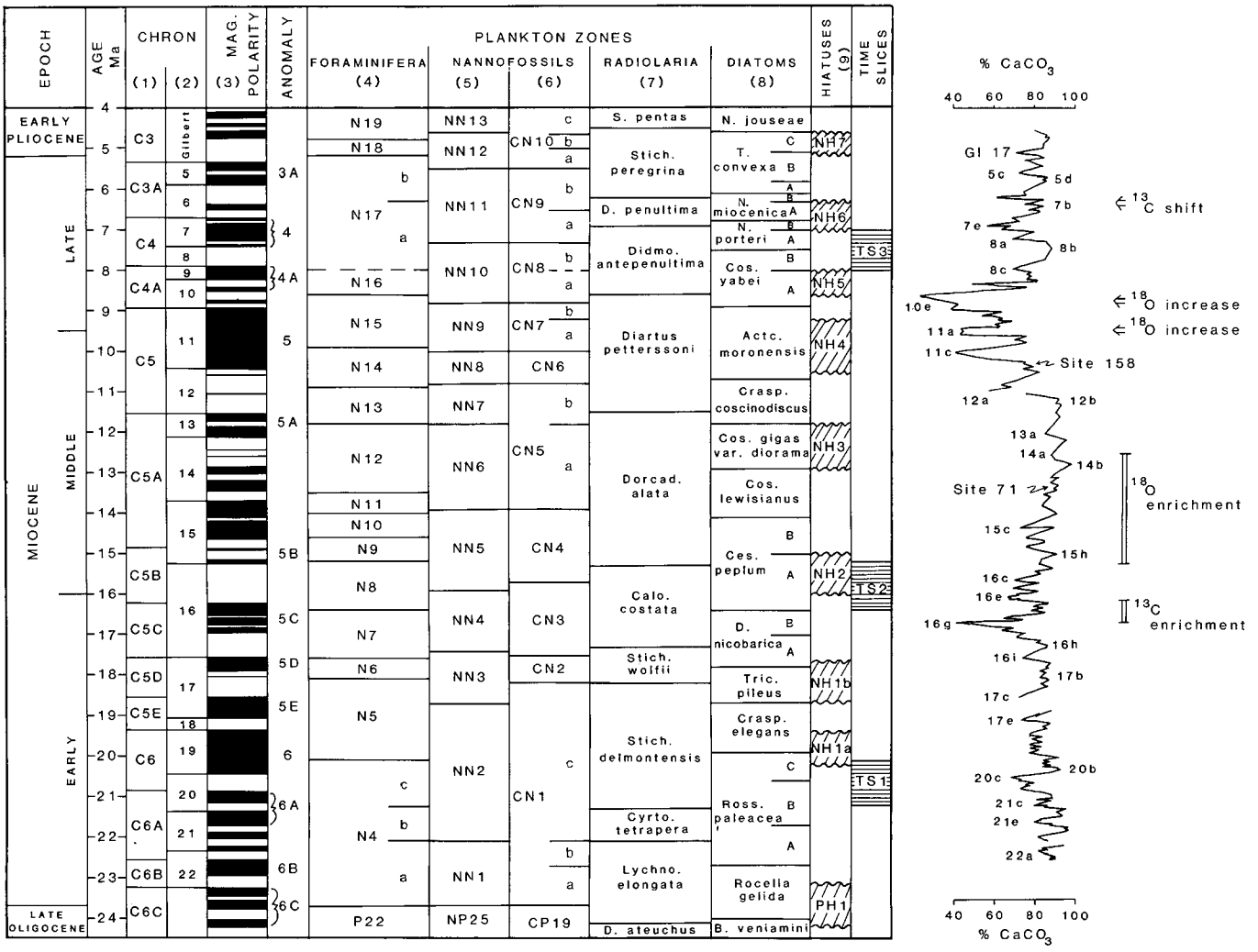

Figure 5. Alternate Miocene time scale derived from a correlation of paleomagnetic Anomaly 5 to paleomagnetic Chron 11 showing correlation of planktonic microfossil zones, widespread deep sea hiatuses, the CENOP time slices, and the percent $CaCO_3$ curve for the eastern equatorial Pacific to the paleomagnetic time scale. Note that differences with Fig. 1 occur between 13.8 and 6.8 Ma. (1) = Tauxe et al., 1983; (2) = LaBrecque et al., 1977 and Theyer and Hammond, 1974; (3) = Berggren et al., 1984; (4) = Blow, 1969; Srinivasan and Kennett, 1981a, b; Keller, in press; (5) = Martini, 1971; (6) = Bukry, 1973, 1975; Okada and Bukry, 1980; (7) = Riedel and Sanfilippo, 1978; (8) = Burckle, 1972; Barron, 1983, in press; and (9) = Keller and Barron, 1983.

as follows: NH 3 (12.9–11.8 Ma), NH 4 (10.5–9.2 Ma), NH 5 (8.6–8.0 Ma), and NH 6 (7.0–6.3 Ma). The major $\delta^{18}O$ enrichment of the middle Miocene has a longer estimated duration, lasting until ~12.5 Ma rather than to ~13.2 Ma in this alternate time scale, and the two $\delta^{18}O$ increases across the middle/late Miocene boundary occur at ~9.5 and 8.8 Ma (Fig. 5). Estimated ages of carbonate events 14b through 7b of Dunn and Moore (1981) also change accordingly (Fig.5) based on replotted sediment accumulation rate plots for Site 71 (Fig. 6) and Site 158.

Barron et al. (in press) notes that utilization of an Anomaly 5-Chron 11 correlation results in sediment accumulation rates that are more uniform during the late Miocene than rates estimated from the traditional time scales which use an Anomaly 5-Chron 9 correlation. Comparison of Figures 2–4 and 6 shows that such a relationship also holds true for DSDP Sites 71 and 289 and to some extent for Site 77. Both the earlier plots for Site 71 (Fig. 2) and Site 289 (Fig. 4) display middle late Miocene rates which are about one-half the rates interpreted for the middle Miocene and latest Miocene at those sites, whereas such a late Miocene kink is not apparent in the later plots (Fig. 6) that utilize the alternate time scale of Figure 5.

Thus, there is good evidence for adopting an Anomaly 5-Chron 11 correlation and accepting the time scale of Figure 5. However, this proposed time scale change is just beginning to be actively debated as this volume goes to press. The papers of this volume have utilized the more traditional time scale of Figure 1

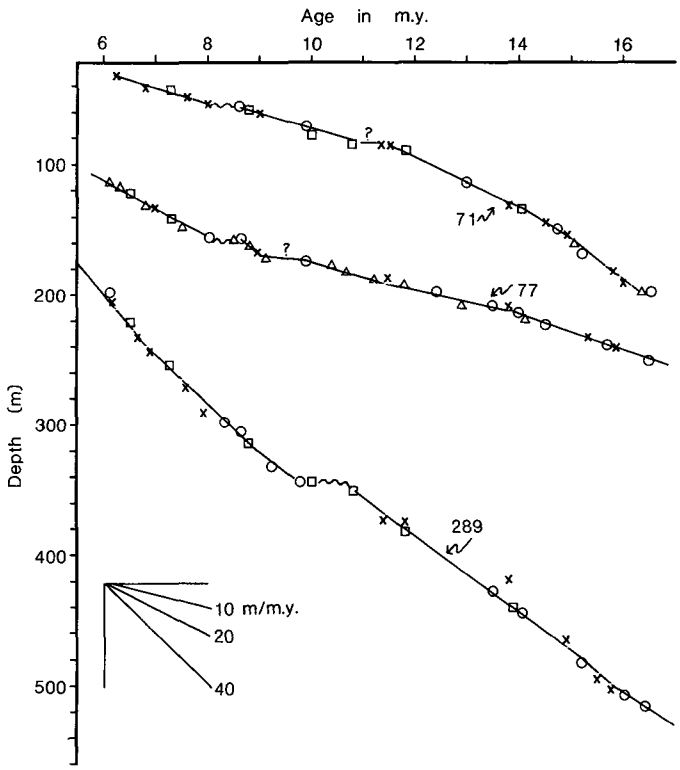

Figure 6. Sediment accumulation plots for the 16 to 6 Ma intervals of DSDP Sites 71, 77, and 289 replotted using the alternate time scale of Figure 5. See Fig. 2 caption for explanation of the symbols.

almost exclusively, but the reader should be able to utilize Tables 1–4 and Figure 5 to redetermine age estimates in this volume should they wish to accept an Anomaly 5-Chron 11 correlation.

ACKNOWLEDGMENTS

We thank David Bukry, Richard Z. Poore, and Charles A. Repenning of the U.S. Geological Survey, Fritz Theyer of the Hawaii Institute of Geophysics, and Bilal Haq of EXXON for their review of this manuscript. W. A. Berggren and D. A. Johnson were helpful in explaining the basis for the alternate time scale utilizing an Anomaly 5-Chron 11 correlation. We also are grateful to CENOP workers for their contributions, especially J. P. Kennett, E. Vincent, L. H. Burckle, K. Romine, and G. Lombari.

REFERENCES CITED

Barron, J. A., 1980, Lower Miocene to Quaternary diatom biostratigraphy of Leg 57, off northeastern Japan, Deep Sea Drilling Project, *in* Initial Reports of the Deep Sea Drilling Project: Washington, U.S. Government Printing Office, v. 56, 57, Part II, p. 641–685.

——1981a, Late Cenozoic diatom biostratigraphy and paleoceanography of the middle latitude eastern North Pacific, Deep Sea Drilling Project Leg 63, *in* Initial Reports of the Deep Sea Drilling Project: Washington, U.S. Government Printing Office, v. 63, p. 507–538.

——1981b, Middle Miocene diatom biostratigraphy of DSDP Site 77B in the eastern equatorial Pacific: Geoscience Journal, v. 2, no. 2, p. 137–144. (Lucknow, India).

——1983, Latest Oligocene through early middle Miocene diatom biostratigraphy of the eastern tropical Pacific: Marine Micropaleontology, v. 7, p. 487–515.

——in press, Miocene to Holocene planktic diatoms; *in* Saunders, J. B., and Bolli, H. M., eds., Biostratigraphy by marine plankton: Cambridge, Cambridge University Press.

Barron, J. A., and Keller, G., 1982, Widespread Miocene deep-sea hiatuses: Coincidence with periods of global cooling: Geology, v. 10, p. 577–581.

——1983, Paleotemperature oscillations in the middle and late Miocene of the northeastern Pacific: Micropaleontology, v. 29, no. 2, p. 150–181.

Barron, J. A., Nigrini, C. A., Pujos, A., Saito, T., Theyer, F., Thomas, E., and Weinreich, N., in press, Synthesis of central equatorial Pacific DSDP leg 85 biostratigraphy: refinement of Oligocene to Quaternary biochronology, *in* Initial Reports of the Deep Sea Drilling Project: Washington, U.S. Government Printing Office, v. 85.

Berggren, W. A., 1981, Correlation of Atlantic, Mediterranean and Indo-Pacific Neogene stratigraphies: Geochronology and chronostratigraphy, *in* Proceedings, IGCP-114 International Workshop on Pacific Neogene Biostratigraphy, Nov. 25-29, 1981, Osaka, Japan, p. 29–60.

Berggren, W. A. and Van Couvering, J. A., 1974, The Late Neogene: biostratigraphy, geochronology, and paleoclimatology of the last 15 million years in marine and continental sequences: Palaeogeography, Palaeoclimatology, and Palaeoecology, v. 16 (1-2), p. 1–216.

——1978, Biochronology, *in* Glassner, G. V. and Hedberg, H. D., eds., Contributions to the geologic time scale: Amer. Assoc. Petrol. Geologists, Studies in Geology, v. 6, p. 39–55.

Berggren, W. A., Aubrey, M. P., and Hamilton, N., 1983, Neogene magnetostratigraphy of Deep Sea Drilling Project Site 516 (Rio Grande Rise, South Atlantic), *in* Initial Reports of the Deep Sea Drilling Project: Washington, U.S. Government Printing Office, v. 72, p. 675–721.

Berggren, W. A., Kent, D. V., and Flynn, J. J., 1984, Paleogene geochronology and chronostratigraphy, *in* Snelling, N. J., ed., Geochronology and the geologic record: Geological Society of London, Special Paper.

Blow, W. H., 1969, Late middle Eocene to recent planktonic foraminiferal biostratigraphy, *in* First International Conference on Planktonic Microfossils, Geneva, 1967, p. 199–421.

Bukry, D., 1973, Low-latitude coccolith biostratigraphic zonation, *in* Initial Reports of the Deep Sea Drilling Project: Washington, U.S. Government Printing Office, v. 15, p. 685–703.

——1975, Coccolith and silicoflagellate stratigraphy, northwestern Pacific Ocean, Deep Sea Drilling Project Leg 32, *in* Initial Reports of the Deep Sea Drilling Project: Washington, U.S. Government Printing Office, v. 32, p. 677–701.

——1981, Cenozoic coccoliths from the Deep Sea Drilling Project: Society of Economic Paleontologists and Mineralogists Special Publication 32, p. 335–353.

Burckle, L. H., 1972, Late Cenozoic planktonic diatom zones from the eastern equatorial Pacific: Beihefte zur Nova Hedwegia, v. 39, p. 217–246.

——1978, Early Miocene to Pliocene diatom datum levels for the equatorial Pacific, *in* Proceedings, Second Working Group Meeting, Biostratigraphic Datum-Planes of the Pacific Neogene, IGCP Project 114: Republic of Indonesia Ministry of Mines and Energy, Directorate General of Mines, Geological Research and Development Center, Special Publication No. 1, p. 25–44.

Burckle, L. H., and Opdyke, N. D., This volume, Latest Miocene/earliest Pliocene diatom correlations in the North Pacific.

Burckle, L. H., Keigwin, L. D., and Opdyke, N. D., 1982, Middle and late Miocene stable isotope stratigraphy: Correlation to the paleomagnetic reversal record: Micropaleontology, v. 28, no. 4, p. 329–334.

Cita, M. B., 1975, The Miocene/Pliocene boundary: History and definition, *in* Saito, T. and Burckle, L. H., eds., Late Neogene epoch boundaries: New York, Micropaleontology Press, p. 1–30.

Dunn, D. A., 1982, Miocene sediments of the equatorial Pacific Ocean: Carbonate stratigraphy and dissolution history [Ph.D. Thesis]: University of Rhode Island, 302 p.

Dunn, D. A., and Moore, T. C., Jr., 1981, Late Miocene/Pliocene (Magnetic Epoch 9-Gilbert Magnetic Epoch) calcium-carbonate stratigraphy of the equatorial Pacific Ocean: Geological Society of America Bulletin, Part II, v. 92, p. 408–451.

Gartner, S., 1973, Absolute chronology of late Neogene calcareous nannofossil succession in the equatorial Pacific: Geological Society of America Bulletin, v. 84, p. 2021–2034.

Gombos, A. M., Jr., 1983, Survey of diatoms in the upper Oligocene and lower Miocene in Holes 515B and 516F, *in* Initial Reports of the Deep Sea Drilling Project: Washington, U.S. Government Printing Office, v. 72, p. 793–804.

Gombos, A. M., Jr., and Ciesielski, P. F., 1983, Late Eocene to early Miocene diatoms from the southwest Atlantic, *in* Initial Reports of the Deep Sea Drilling Project: Washington, U.S. Government Printing Office, v. 71, p. 583–634.

Haq, B. U., 1980, Biogeographic history of Miocene calcareous nannoplankton and paleoceanography of the Atlantic Ocean: Micropaleontology, v. 26, no. 4, p. 414–443.

Haq, B. U. Worsley, J. R., Burckle, L. H., Douglas, R. G., Keigwin, L. D., Opdyke, N. D., Savin, S. M., Sommer, M. A., Vincent, E., and Woodruff, F., 1980, Late Miocene marine carbon-isotope shift and synchroneity of some phytoplanktic biostratigraphic events: Geology, v. 8, p. 427–431.

Hsu, K. J., LaBrecque, J. L., and the shipboard scientific party, 1984, Site 519, *in* Initial Reports of the Deep Sea Drilling Project: Washington, U.S. Government Printing Office, v. 73, p. 27–93.

Jenkins, D. G., and Orr, W. N., 1972, Planktonic foraminiferal biostratigraphy of the eastern equatorial Pacific, Leg 9, *in* Initial Reports of the Deep Sea Drilling Project: Washington, U.S. Government Printing Office, v. 9, p. 1059–1196.

Johnson, D. A., and Wick, B. J., 1982, Precision of correlation of radiolarian datum levels in the middle Miocene equatorial Pacific: Micropaleontology, v. 28, no. 1, p. 1–30.

Keigwin, L. D., Jr., 1979, Late Cenozoic stable isotope stratigraphy and paleoceanography of DSDP site from the east equatorial and central north Pacific Ocean: Earth and Planetary Science Letters, v. 45, p. 361–382.

Keller, G., 1980a, Early to middle Miocene planktonic foraminiferal datum levels of the equatorial and subtropical Pacific: Micropaleontology, v. 26, no. 4, p. 372–391.

——1980b, Middle to late Miocene planktonic foraminiferal datum levels and paleoceanography of the north and southeastern Pacific Ocean: Marine Micropaleontology, v. 5, p. 249–281.

——1981a, Miocene biochronology and paleoceanography of the North Pacific. Marine Micropaleontology, v. 6, p. 535–551.

——1981b, Planktonic foraminiferal faunas of the equatorial Pacific suggest early Miocene origin of present oceanic circulation: Marine Micropaleontology, v. 6, p. 269–295.

——in press, The Oligocene/Miocene boundary in the equatorial Pacific, *in* Steiniger, F., and Gelati, R., eds., In search of the Palaeogene/Neogene boundary stratotype, Part 2, Rivista Italiana de Paleontologia e Stratigraphia.

Keller, G., this volume, Depth stratification of planktonic foraminifera in the Miocene Ocean.

Keller, G., and Barron, J. A., 1981, Integrated planktic foraminiferal and diatom biochronology for the northeast Pacific and the Monterey Formation, *in* Garrison, R. E., and Douglas, R. G., eds., The Monterey Formation and related siliceous rocks of California: Los Angeles, Calif., Pacific Section Society of Economic Paleontologists and Mineralogists, p. 43–54.

——1983, Paleoceanographic implications of Miocene deep-sea hiatuses: Geological Society of America Bulletin, v. 94, p. 590–613.

Keller, G., Barron, J. A., and Burckle, L. H., 1982, North Pacific late Miocene correlations using microfossils, stable, isotopes, percent Ca CO_3, and magnetostratigraphy: Marine Micropaleontology, v. 7, p. 327.

Kennett, J. P., 1977, Cenozoic evolution of Antarctic glaciation, the circum-Antarctic Ocean, and their impact on global paleoceanography: Journal of Geophysical Research, v. 82, no. 27, p. 3843–3860.

La Brecque, J. L., Kent, D. V., and Cande, S. C., 1977, Revised magnetic polarity time scale for the Cretaceous and Cenozoic. Geology, v. 5, p. 330–335.

Loutit, T. S., and Kennett, J. P., 1979, Application of carbon isotope stratigraphy to late Miocene shallow marine sediments, New Zealand: Science, v. 24, p. 1196–1199.

Mankinen, E. A., and Dalrymple, G. B., 1979, Revised geomagnetic polarity time scale for the interval 0-5 m.y. B.P.: Journal of Geophysical Research, v. 84, no. B2, p. 615–626.

Matthews, R. K., and Poore, R. Z., 1980, Tertiary ^{18}O record and glacioeustatic sea-level fluctuations: Geology, v. 8, p. 501–504.

Martini, E., 1971, Standard Tertiary and Quaternary calcareous nannoplankton zonation, *in* Farinacci, A., ed., Proceedings of the II Planktonic Conference Roma 1970: Rome, Edizioni Tecnoscienza, v. 2, p. 739–777.

Moore, T. C., Jr., and Lombari, G., 1981, Sea surface temperature changes in the North Pacific during the late Miocene: Marine Micropaleontology, v. 6, no. 5–6, p. 581–597.

Okada, H., and Bukry, D., 1980, Supplementary modification and introduction of code numbers to the low-latitude coccolith biostratigraphic zonation (Bukry 1973; 1975): Marine Micropaleontology, v. 5, p. 321–325.

Poore, R. Z., 1981, Late Miocene biogeography and paleoclimatology of the central North Atlantic: Marine Micropaleontology, v. 6, p. 599–616.

Poore, R. Z., Tauxe, L., Percival, S. F., Jr., LaBrecque, J. L., Wright, R., Petersen, N. P., Smith, C. C., Tucker, P., and Hsu, K. J., 1983, Late Cretaceous-Cenozoic magnetostratigraphic and biostratigraphic correlations of the South Atlantic Ocean: DSDP Leg 73: Palaeogeography, Palaeoclimatology, Palaeoecology, v. 42, p. 127–149.

——1984, Late Cretaceous-Cenozoic magnetostratigraphic and biostratigraphic correlations of the South Atlantic Ocean, Deep Sea Drilling Project Leg 73, *in* Initial Reports of the Deep Sea Drilling Project: Washington, U.S. Government Printing Office, v. 73, p. 645–655.

Riedel, W. R., and Sanfilippo, A., 1978, Stratigraphy and evolution of tropical Cenozoic radiolarians: Micropaleontology, v. 24, no. 1, p. 61–96.

Romine, K., this volume, Radiolarian biogeography and paleoceanography of the North Pacific at 8 MA.

Ryan, W.B.F., Cita, M. B., Rawson, M. D., Burckle, L. H., and Saito, T., 1974, A paleomagnetic assignment of Neogene stage boundaries and the development of isochronous datum planes between the Mediterranean, the Pacific and Indian Oceans in order to investigate the response of the world ocean to the Mediterranean "salinity crisis": Rivista Italiana Paleontologia, v. 80, p. 631–688.

Saito, T., 1977, Late Cenozoic planktonic foraminiferal datum levels: the present state of knowledge toward accomplishing pan-Pacific stratigraphic correlation, *in* Proceedings, First International Congress on Pacific Neogene Stratigraphy, Tokyo, 1976: Tokyo, Kaiyo Shuppan Co., p. 61–80.

Saito, T., Burckle, L. H., and Hays, J. D., 1975, Late Miocene to Pleistocene biostratigraphy of equatorial Pacific sediments, *in* Saito, T., and Burckle, L. H., eds., Late Neogene epoch boundaries: New York, Micropaleontology Press, p. 226–244.

Savin, S. M., Douglas, R. G., Keller, G., Killingley, J. S., Shaughnessy, L., Sommer, M. A., Vincent, E., and Woodruff, F., 1981, Miocene benthic foraminiferal isotope records: a synthesis: Marine Micropaleontology, v. 6, p. 423–450.

Shackleton, N. J., and Kennett, J. P., 1975, Paleotemperature history of the Cenozoic and the initiation of Antarctic glaciation: Oxygen and carbon isotope analyses in DSDP Sites 277, 279, and 281, *in* Initial Reports of the Deep Sea Drilling Project: Washington, U.S. Government Printing Office, v. 29, p. 743–755.

Shafik, S., 1975, Nannofossil biostratigraphy of the southwest Pacific, Deep Sea Drilling Project, Leg 30, *in* Initial Reports of the Deep Sea Drilling Project: Washington, U.S. Government Printing Office, v. 30, p. 549–598.

Shaw, A. B., 1964, Time in stratigraphy: New York, McGraw-Hill, 365 p.

Srinivasan, M. S., and Kennett, J. P., 1981a, A review of Neogene planktonic

foraminiferal biostratigraphy: Applications in the equatorial and South Pacific, *in* Deep Sea Drilling Project: A decade of progress: Society of Economic Paleontologists and Mineralogists, Special Publication, no. 32, p. 395–432.

——1981b, Neogene planktonic foraminiferal biostratigraphy and evolution: equatorial to subantarctic South Pacific: Marine Micropaleontology, v. 6, p. 499–533.

Tauxe, L., Tucker, P., Petersen, N. P., and LaBrecque, J. P., 1983, The magnetostratigraphy of Leg 73 sediments: Palaeogeography, Palaeoclimatology, Palaeocology, v. 42, p. 65–90.

Theyer, F. and Hammond, S. R., 1974, Paleomagnetic polarity sequence and radiolarian zones, Brunhes to Epoch 20: Earth Planetary Science Letters, v. 22, p. 307–319.

Theyer, F., Mato, C. Y., and Hammond, S. R., 1978, Paleomagnetic and geochronologic calibration of latest Oligocene to Pliocene radiolarian events, equatorial Pacific: Marine Micropaleontology, v. 3, p. 377–395.

Thunell, R. C., 1981, Late Miocene-early Pliocene planktonic foraminiferal biostratigraphy and paleoceanography of low-latitude marine sequences: Marine Micropaleontology, v. 6, p. 71–90.

Vincent, E., 1981a, Neogene planktonic foraminifers from the central North Pacific, Deep Sea Drilling Project Leg 62, *in* Initial Reports of the Deep Sea Drilling Project: Washington, U.S. Government Printing Office, v. 62, p. 329–353.

——1981b, Neogene carbonate stratigraphy of Hess Rise (central North Pacific) and paleoceanographic implications, *in* Initial Reports of the Deep Sea Drilling Project: Washington, U.S. Government Printing Office, v. 62, p. 571–606.

Vincent, E., Killingley, J. S., and Berger, W. H., 1980, The magnetic epoch 6 carbon shift: A change in the ocean's $^{13}C/^{13}C$ ratio 6.2 million years ago: Marine Micropaleontology, v. 5, no. 2, p. 185–203.

Vincent, E. and Killingley, J. S., in press, Lower and middle Miocene isotope stratigraphy at DSDP Sites 573, 574, and 575, central equatorial Pacific, *in* Initial Reports of the Deep Sea Drilling Project: Washington, U.S. Government Printing Office, v. 85, p. 000–000.

Westberg, M. J., and Riedel, W. R., 1978, Accuracy of radiolarian correlations in the Pacific Miocene: Micropaleontology, v. 24, p. 1–23.

Woodruff, F., Savin, S. M., and Douglas, R. G., 1981, Miocene stable isotope record: A detailed deep Pacific Ocean study and its paleoclimatic implications: Science, v. 212, p. 665–668.

MANUSCRIPT ACCEPTED BY THE SOCIETY DECEMBER 17, 1984

Printed in U.S.A.